

---

Masters Theses

Student Theses and Dissertations

---

1965

## An evaluation of the feasibility of neutron microradiography

Maynard L. Arment

Follow this and additional works at: [https://scholarsmine.mst.edu/masters\\_theses](https://scholarsmine.mst.edu/masters_theses)

 Part of the [Nuclear Engineering Commons](#)

Department: Mining and Nuclear Engineering

---

### Recommended Citation

Arment, Maynard L., "An evaluation of the feasibility of neutron microradiography" (1965). *Masters Theses*. 6956.

[https://scholarsmine.mst.edu/masters\\_theses/6956](https://scholarsmine.mst.edu/masters_theses/6956)

This thesis is brought to you by Scholars' Mine, a service of the Curtis Laws Wilson Library at Missouri University of Science and Technology. This work is protected by U. S. Copyright Law. Unauthorized use including reproduction for redistribution requires the permission of the copyright holder. For more information, please contact [scholarsmine@mst.edu](mailto:scholarsmine@mst.edu).

AN EVALUATION OF THE FEASIBILITY  
OF NEUTRON MICRORADIOGRAPHY

BY

MAYNARD L. ARMENT

---

A

THESIS

submitted to the faculty of the

UNIVERSITY OF MISSOURI AT ROLLA

in partial fulfillment of the requirements for the

Degree of

MASTER OF SCIENCE IN NUCLEAR ENGINEERING



Rolla, Missouri

1965

---

Approved by

  
\_\_\_\_\_  
Wm. H. D. [unclear]  
(advisor)

  
\_\_\_\_\_  
  
\_\_\_\_\_

Abstract

The metal working industry has used metallography and micro-radiography extensively in the past decade. X-ray or gamma micro-radiography has several advantages as compared to metallography, but a disadvantage concerning alloys of adjacent elements; microradiography cannot distinguish between elements 2 or less atomic numbers apart. Attempts were made using neutron microradiography to distinguish between cadmium and tin rich grains. A maximum resolution of 0.017 inches was found with a calculated possibility of a resolution less than 0.002 inches.

Acknowledgements

The author wishes to thank Dr. D. S. Eppelsheimer, Professor of Metallurgical Engineering and Nuclear Engineering and Chairman of the Nuclear Advisory Committee, for his encouragement and assistance during the course of this investigation. He also wishes to thank Dr. D. R. Edwards and the UMR reactor staff for their assistance.

Thanks are extended to the Department of Metallurgical Engineering and the Department of Geology for the use of their equipment.

The author is grateful for the materials supplied by the Indium Company of America, New York, New York and the American Smelting and Refining Company, St. Louis, Missouri. He is also grateful for the financial assistance received from the Atomic Energy Commission as a Nuclear Science and Engineering Fellow.



Table of Contents

	Page
Title Page.....	i
Abstract.....	ii
Acknowledgements.....	iii
Table of Contents.....	iv
List of Figures.....	vi
List of Tables.....	viii
I. Introduction.....	1
II. Literature Review.....	7
III. Experimental Procedure.....	9
Preparation of Cd-Sn Alloys.....	9
Preparation of Thin Sections.....	10
Preparation for Irradiation.....	10
Irradiation.....	13
Photographic Plate Exposure.....	13
Development of Plates and Films.....	13
Production of Radiographs and Microradiographs.....	13
Examination of the Microradiographs and Radiographs..	14
Metallographic Supplement.....	15
IV. Data and Results.....	18
V. Discussion.....	24
VI. Conclusion.....	43
VII. Summary.....	46
VIII. Recommendations.....	47

Table of Contents (Cont.)

	Page
IX. Appendix 1.....	48
Materials.....	48
Equipment.....	48
X. Appendix 2.....	50
XI. Appendix 3.....	51
XII. Appendix 4.....	52
XIII. Appendix 5.....	55
XIV. Appendix 6.....	56
XV. Appendix 7.....	57
XVI. Bibliography.....	59
XVII. Vita.....	60

List of Figures

	Page
Figure 1. Differential Absorption.....	3
Figure 2. Variation with Wavelength of Mass Absorption Coefficient (Schematic).....	4
Figure 3. Absorption Characteristics of Two Materials (Schematic).....	5
Figure 4. Samples on Transfer Sheet.....	12
Figure 5. Assembly in Position.....	12
Figure 6. Furnace Cooled Alloy.....	16
Figure 7. Air Cooled Alloy.....	16
Figure 8. Air Dropped Alloy.....	17
Figure 9. Reactor Run 27.....	30
Figure 10. Cadmium and Tin Turnings.....	30
Figure 11. Reactor Run 9.....	31
Figure 12. Reactor Run 18.....	31
Figure 13. Reactor Run 18.....	32
Figure 14. Reactor Run 18.....	32
Figure 15. Reactor Run 23.....	33
Figure 16. Reactor Run 23.....	33
Figure 17. Reactor Run 24.....	34
Figure 18. Reactor Run 24.....	34
Figure 19. Reactor Run 25.....	35
Figure 20. Reactor Run 26.....	35
Figure 21. Reactor Run 26.....	36
Figure 22. Reactor Run 27.....	36

List of Figures (Cont.)

	Page
Figure 23. Reactor Run 27.....	37
Figure 24. Reactor Run 27.....	37
Figure 25. Reactor Run 27.....	38
Figure 26. Reactor Run 28.....	39
Figure 27. Reactor Run 28.....	39
Figure 28. Reactor Run 30.....	40
Figure 29. Reactor Run 30.....	40
Figure 30. Reactor Run 30.....	41
Figure 31. Reactor Run 30.....	41
Figure 32. Reactor Run 30.....	42

List of Tables

	Page
Table 1. Sample Description.....	11
Table 2. Data.....	19
Table 3. Results.....	22

## I. Introduction

The physical properties of an alloy or metal are dependent to a large extent upon the internal microstructure of the material. Therefore, methods of microstructure examination have assumed an important role in metallurgical engineering today.

One of the more recent examination methods developed for opaque materials is that of microradiography<sup>1,2,3,4,5</sup> using either x-rays or gamma rays. The basis of this technique is the modification of the radiation intensity as it penetrates a thin section of heterogeneous material. This phenomenon of differential absorption (Fig. 1) is dependent upon the linear absorption coefficients of the differential areas through which the radiation is penetrating. If the degree of modification varies greatly between adjacent areas, the differential absorption is large; the larger the differential absorption, the greater the resolution obtainable.

The linear absorption coefficient is dependent upon essentially two processes; the true absorption caused by electronic transitions within the atom and the scattering of x-rays considered as removal from the transmitted beam. The scattering of x-rays is considered negligible for all except the very light elements.

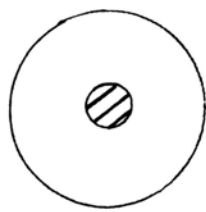
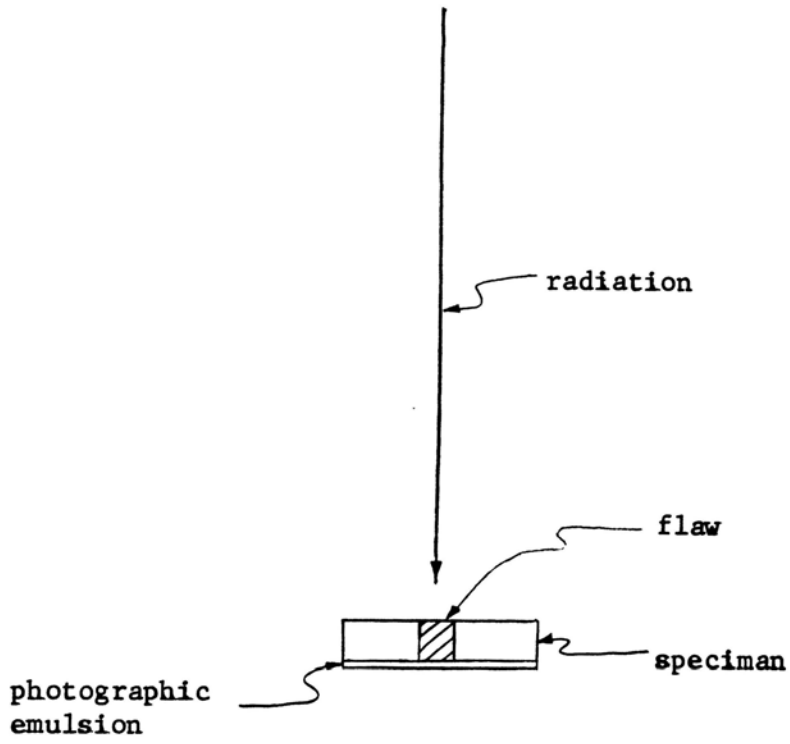
True absorption is the interaction of an electron and an x-ray in which the x-ray disappears and the electron is ejected from its shell in the atom. An atom with this electron vacancy will emit characteristic radiation which radiates in all directions. To eject an electron, the energy of the x-ray must exceed a certain minimum value. When the energy of the x-ray equals the minimum required, a relative maximum absorption coefficient exists (Fig. 2); this is referred to as an

absorption edge. If the energy of the x-ray exceeds the energy required for the removal of the electron, the probability of the x-ray penetrating the atom increases; this accounts for the existence of the relative maximum. There are absorption edges (Fig. 2) existing for each of the quantum levels within the atom.

An alloy may be examined by x-ray microradiography if the difference between the linear absorption coefficients is relatively great. If the difference is not great enough (<20%) for most wavelengths, x-ray microradiography may still be used if the bombarding radiation has a wavelength equal to or a little less than that of an absorption edge of one of the materials in the alloy. This would allow one linear absorption coefficient to be much greater than the other (Fig. 3).

If the alloy has two elements which are within two atomic numbers of each other, then the linear absorption<sup>6</sup> coefficient difference<sup>1</sup> will be small. If x radiation with a wavelength corresponding to an absorption edge cannot be found (considering conventional target radiation), then the alloy cannot be examined by ordinary microradiography.

The object of this thesis is to determine the possibility of using neutrons as the penetrating radiation for alloys which could not be examined by standard microradiographic radiations. The use of a neutron beam, however, imposes a limitation in that at least one of the alloy constituents should have a neutron absorption cross-section several order of magnitude larger than those of the other constituents for high resolution.



Speciman

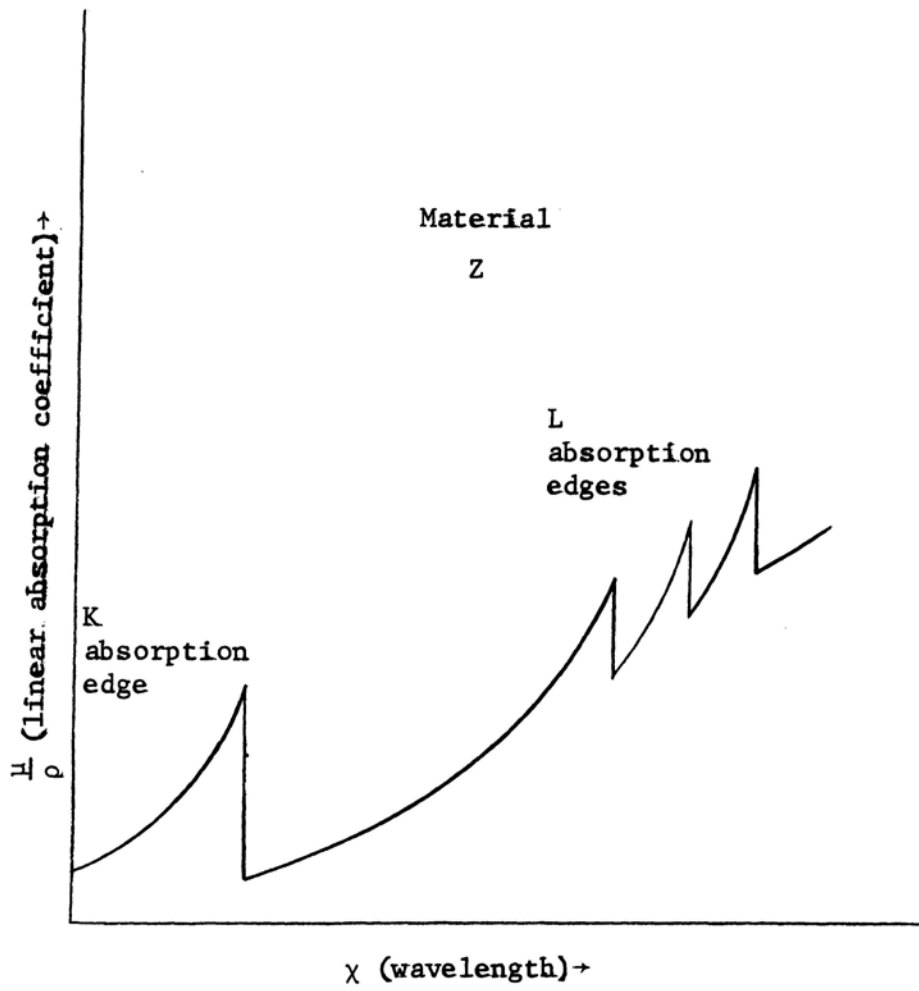


Negative

Differential Absorption

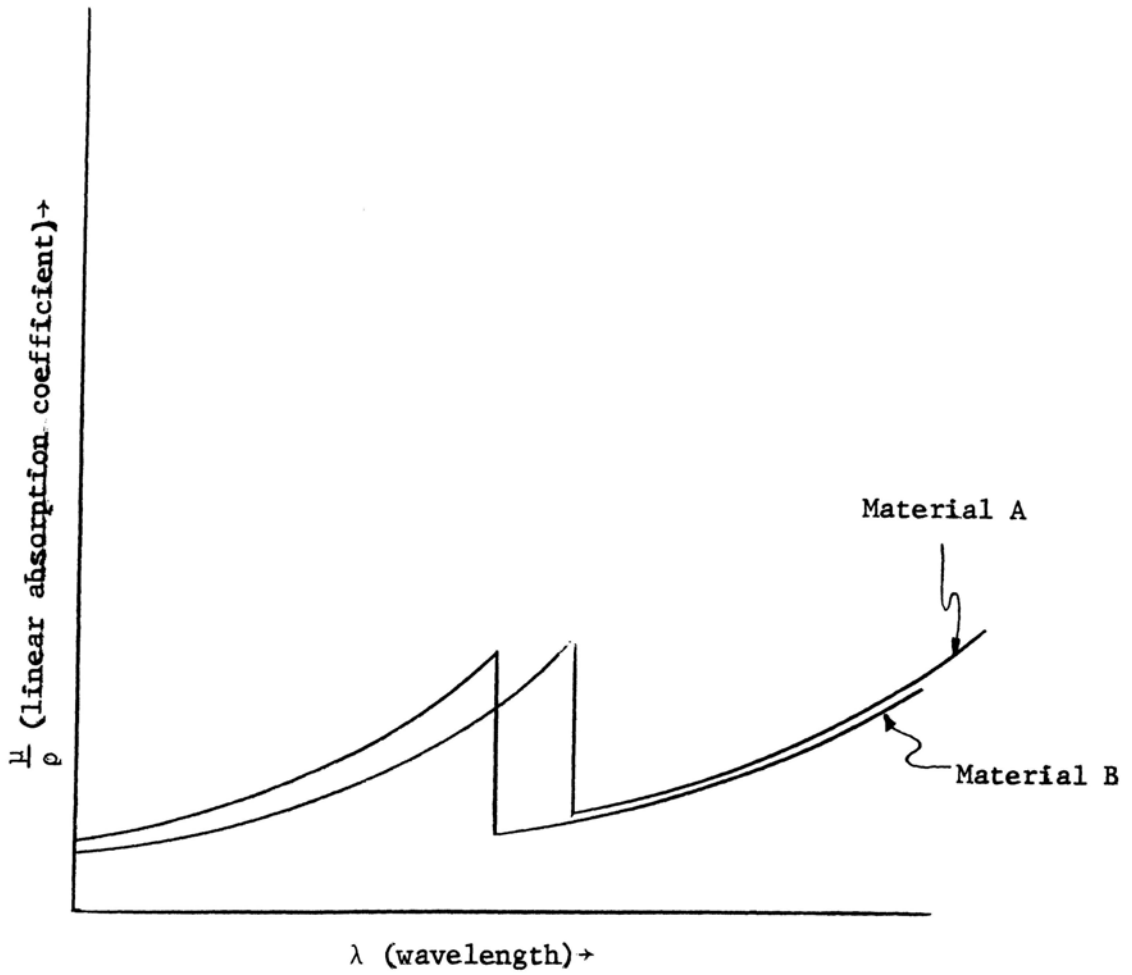
Figure 1





Variation with Wavelength of  
Mass Absorption Coefficient (Schematic)

Figure 2



Absorption Characteristics of Two Materials (Schematic)

Figure 3

The alloy chosen which met these requirements was the eutectic of the cadmium-tin system (39.25% Cd)\*. It was decided to examine these alloys at three cooling rates: (1) furnace cooled, three hours from 400°C to 23°C; (2) air cooled, 30 minutes from 400°C to 23°C; and (3) air dropped, 10 seconds from 400°C to 23°C.

Cadmium and tin have similar atomic numbers, 48 and 50 respectively, but natural cadmium has a nuclear absorption cross-section of 2450\* barns while that of tin is 0.60\*\* barns (These cross-sections are for neutrons which have a velocity of 2,200 m/sec, i.e., "thermal" neutrons).

\*Metals Handbook, American Society of Metals, 1948.

\*\*Handbook of Chemistry and Physics, Chemical Rubber Publishing Company, 44 Edition, 1963.

## II. Literature Review

The study of the internal structure has been performed by many methods; however, with regard to this thesis, this review will be confined to those methods using radiographic or microradiographic techniques.

An examination of the microstructure of an alloy using microradiographic methods requires a sample thinned such that the differential absorption across the sample depends upon the individual grain and microflaw absorption. If it is considered that the differential absorption of a microheterogeneous sample with a thickness of many (>50) grain diameters is essentially zero and that of the same sample infinitely this is also zero, then if any differential absorption optimum exists, it must exist between these limits. This optimum differential absorption for microradiography must be dependent upon the size of the microfeature of interest to the observer. From x-ray microradiographs and data in Votava<sup>7</sup>, et al, the optimum range of sample thickness was determined to be equal to  $1.0 \pm 0.5$  of the average grain diameter. This relation to grain size was utilized for this thesis because of the absorption functions using either neutrons or x-rays. In both instances the intensity of the emerging radiation varies as an exponential function of the distance, through the material, traveled by the radiation.

At Argonne National Laboratory, Berger<sup>8</sup> and Beck<sup>9</sup> have been producing neutron radiographs of uranium fuel pins to determine the extent and size of macroscopic voids. These investigators have used a procedure which shall be referred to as the transfer method; this method was utilized in this thesis. Their transfer method involved the use of recorder sheets to record the differential absorption of the neutrons

by the sample. These sheets consisted of materials with a high neutron cross-section and a subsequent radioactive decay of the order of one hour. To obtain a permanent visual record of the samples, the recorder sheet was placed against an x-ray film; the radioactive decay of the neutron activated nuclei exposed the plate.

Berger and Beck's procedure consisted of using indium, dysprosium, or silver recorder sheets (0.1 inches thick) and placing these in contact with a uranium fuel pin (1.44 inches in diameter). This assembly was placed at a right angle to a unidirectional neutron beam as to allow the neutrons which penetrated the sample to impinge upon the recorder sheet. With a typical sample, after seven minutes in a flux of  $9 \times 10^{+7}$  neutrons/cm<sup>2</sup>/sec, the assembly was removed, and the recorder sheet was placed in an x-ray film cassette in contact with Kodak AA x-ray film. The dysprosium was allowed to expose the film for 6.9 hours (approximately three half-lives of Dy<sup>165</sup>). The film was then developed by standard radiographic procedures.

The film exposure time is directly proportional to the half-life of the decaying species of the recorder sheet. To obtain an exposure within a reasonable length of time it is necessary that the half-life of the nucleus be eight hours or less. This will insure that the film can be sufficiently exposed within one day. Also the minimum half-life should be larger than the time elapsed from the irradiation facility to the film; this would insure a high recorder sheet activity when the film is exposed.

Another limiting factor in the choice of recorder sheet materials is the reaction cross-section. The activity at the end of irradiation varies directly as the cross-section; therefore, the greater the cross-section, the shorter the film exposure time.

### III. Experimental Procedure

#### Materials and Equipment

A complete list of the materials and equipment used in this thesis project are in Appendix 1.

Preparation of Cd-Sn Alloys: A Cd-Sn alloy containing  $39.25 \pm 0.2\%$  Cd was prepared by mixing 150 grams of Cd and 232.15 grams of Sn. The mixture was added to a fire clay crucible and completely covered with ground charcoal to prevent oxidation. The crucible was placed in an electric furnace and heated to a temperature of  $400^{\circ}\text{C}$  for four hours. The alloy was then cooled to below the fusion temperature, held below the fusion temperature for 30 minutes and the temperature of the alloy again was raised to  $400^{\circ}\text{C}$ . This process was repeated twice; during the final cooling, a thermocouple circuit was used to give cooling curve data, which indicated that the alloy was of eutectic composition (39.25% Cd). The alloy was then heated to  $400^{\circ}\text{C}$  and allowed to furnace cool to room temperature.

Two other alloys of the same composition were prepared in a similar manner with the exception of the final cooling rate. The first of these alloys was removed from the furnace and allowed to air cool within the crucible. The final cooling of the other alloy was as follows: molten metal was pipetted from the crucible, and drops\* of the alloy were allowed to fall onto a metallographically polished aluminum plate from a height of 6 inches.

\*These shall be referred to as "drop cooled".

Preparation of Thin Sections: After the specimens were examined metallographically, they were mounted on glass microscope slides using Canada balsam with the etched face on the slide. The area opposite the etched face was rough polished on 240, 320, 400, and 600 wet SiC papers, respectively, until the approximate desired thickness was obtained. The specimens were then fine polished with Linde B alumina on billiard cloth and etched with 5% nital.

The average thicknesses were then calculated by using the following equation:

$$t = \frac{\text{mass}}{\text{density} \times \text{area}}$$

The thicknesses are tabled in Table 1.

Preparation for Irradiation: The thinned sections were each placed on the indium face of a recorder sheet\* (Appendix 5). The function of the indium was to record, temporarily, the differential absorption across the sample.

A glass microscope slide was placed over each section to insure sample and indium contact. A gum rubber band was placed around this assembly to prevent movement of component parts (Fig. 4).

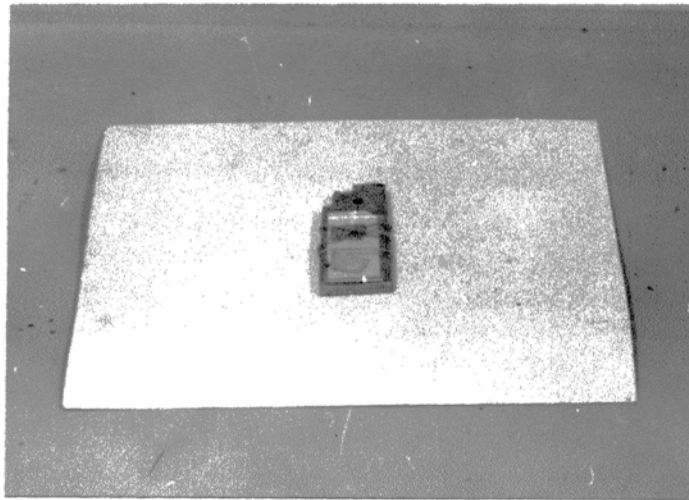
One or two of these assemblies were mounted on a 4 inch x 8 inch x 0.25 inch cadmium sheet which minimized neutron backscatter and placed within two inches of the graphite thermal column (Fig. 5). This placed the sample approximately 5.5 feet from the reactor core (neutron source) with 5 feet of graphite between the core and the sample thus being in position to allow a unidirectional thermal flux to impinge upon the assembly.

Table 1Sample Descriptions

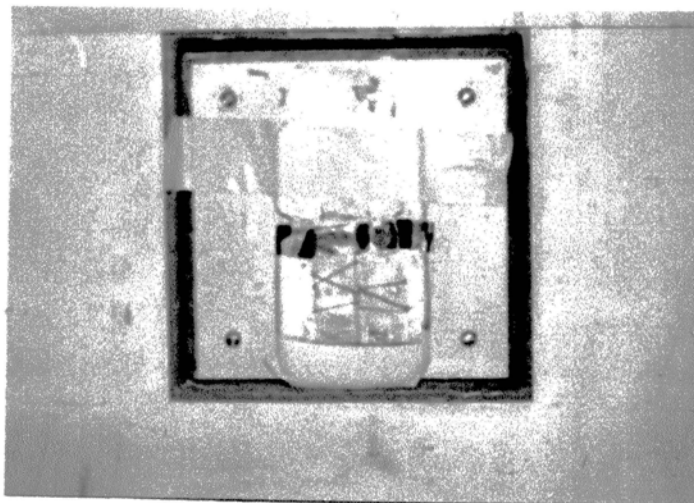
<u>Sample No.</u>	<u>Heat Treatment</u>	<u>*Average Thickness (in.) ± .0001 in.</u>
1A	furnace cooled	0.0049
1B	furnace cooled	0.0067
1C	furnace cooled	0.0045
2A	air cooled	0.0022
2B	air cooled	0.0009
2C	air cooled	0.0012
3A	air dropped	0.00049
3B	air dropped	0.0016
3C	air dropped	0.00077

\*See Appendix 2





Samples on Transfer Sheet (1/5 actual size)  
Figure 4



Assembly in Position (1/8 actual size)  
Figure 5

Irradiation: With the entire assembly in place, the reactor was operated at a power of 10 Kw. The samples were irradiated for times varying from 6 to 104 minutes (Table 2). The flux at the sample position at the end of the thermal column was  $2.38 \times 10^6$  n/cm<sup>2</sup>/sec (Appendix 3).

Photographic Plate Exposure: Within 1.5 hours after irradiation, the recorder sheet was removed from the assembly and placed such that the indium was in intimate contact with the film or plate emulsion. The time used was of such a duration as to allow adequate film exposure. The activated indium nuclei were allowed to expose the film for times ranging from approximately 1 to 8 hours (Table 2).

Development of Plates and Films: The Kodak Metallographic plates, the Kodak High Resolution plates, and the Kodak Spectroscopic films (all single emulsion) were developed in Kodak D-19 at  $60 \pm 1^\circ\text{C}$  for seven minutes, placed in shortstop for 20 seconds, and fixed for five minutes in Kodak F-5. The Dupont Fine Grained Industrial X-ray film (double emulsion) was developed in Kodak X-ray Developer at  $68 \pm 1^\circ\text{C}$  for five minutes, agitated in shortstop for 20 seconds, and fixed in Kodak X-ray Fixer for five minutes.

The development of each of the plates or films was of high importance for the retention of maximum contrast and resolution. For these reasons, the plates and film were developed in solutions which would give the highest attainable contrast.

Production of Radiographs and Microradiographs: The contact prints (radiographs) were produced by an exposure of from 0.5 to 3.0 seconds using a blue-light contact printer with F-4 paper. They were then developed in a mixture composed of Kodak D-72 stock solution and water

in a 21 to 2 ratio; the prints were developed in 45 seconds at 60°C. The prints were then agitated in shortstop for 30 seconds and fixed in Kodak F-5 for five minutes.

The microradiographs were produced by using a Leitz Focomatic enlarger with an El Nikkon 5 cm f/2.8 lens. The prints were developed in a manner identical to that used for the contact enlargement.

Proper technique is required for the developing and fixing of the radiographs and microradiographs. The paper, enlarger or printer, and solutions must be of high quality.

Examination of the Microradiographs and Radiographs: Each of the radiographs and microradiographs were examined for resolution with a 10X magnifier with a scale of 0.01 mm divisions. The maximum visible resolution was found by scanning each radiograph until the three smallest cadmium rich areas were found. The diameters of these areas were averaged to obtain the maximum visible resolution (M.R.).

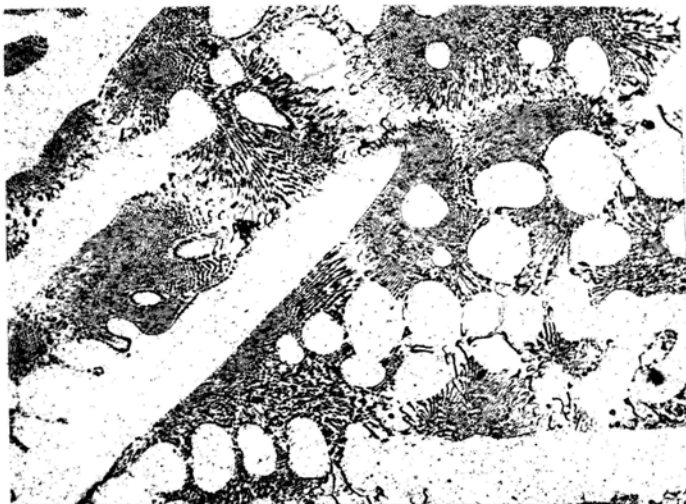
Metallographic Supplement: Three specimens from each sample were prepared by the standard metallographic methods using Linde B alumina abrasive for the final polish. The polished specimens were chemically etched with a solution of 5% nitric acid and 95% methyl alcohol (5% nital).

In the photomicrographs, the cadmium rich areas are dark and those rich in tin are light. The photomicrographs shown are characteristic of each alloy.

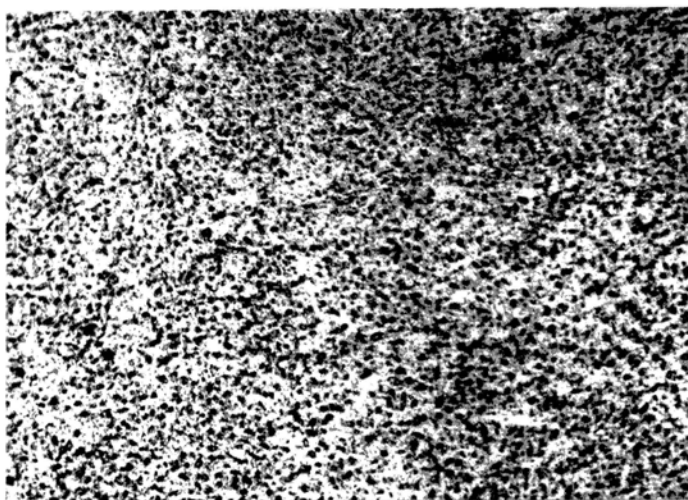
Figure 6 is a photomicrograph of the furnace cooled alloy. It illustrates the circular and elongated tin rich grains imbedded in a matrix of cadmium rich material. The grain sizes vary from less than 0.001 to .1 inches.

Figure 7 is a photomicrograph of an air cooled sample. The grain size is small and the shapes are circular.

The photomicrograph (Fig. 8) of the air-dropped alloy illustrates an extremely small grain size.



39.25% Cd - 60.75% Sn  
Furnace Cooled Alloy 75X  
Figure 6



39.25% Cd - 60.75% Sn  
Air Cooled Alloy 50X  
Figure 7



39.25% Cd - 60.75% Sn  
Air Dropped Alloy 200X  
Figure 8

#### IV. Data and Results

Tables 1, 2, and 3 show the data and results for each reactor run. Figures 9 through 32 are neutron microradiographs or radiographs of certain of the experiments.

In Table 3 MR refers to the maximum visible resolution (previously described),  $D_0$  refers to the distance between the prongs on area 1 at a distance of 0.01 inches from their intersection point, and  $D_H$  refers to the distance between the tines of area 2 at a distance of 0.01 inches from their intersection point. Area 1 is the two pronged dark (Cd rich) area situated such that one of the prongs extends into the flaw of Sample 1A. Area 2 was the horseshoe shaped area approximately 0.25 inches from the flaw of Sample 1A.

The column titled Decay Time refers to the time the irradiation ended to the beginning of the film or plate exposure. All other columns are self explanatory.

Table 2

Data

<u>Reactor Run No.</u>	<u>Irradiation Time* (Min.) ± .5 min.</u>	<u>Decay Time (Min.) ± 1 min.</u>	<u>Film Exposure Time (Min.) ± 1 min.</u>	<u>Type of Film or Plate</u>
1	104.2	135	120	Kodak Spectroscopic 649-0
2	104.2	75	120	Kodak Spectroscopic 649-0
3	10.4	75	120	Kodak Spectroscopic 649-0
4	104.2	150	960	Kodak Spectroscopic 649-0
5	240	300	540	Kodak Spectroscopic 649-0
6	10	40	175	Dupont Fine Grain Industrial X-ray Film
7	10	43	170	Dupont Fine Grain Industrial X-ray Film
8	10	64	135	Dupont Fine Grain Industrial X-ray Film
9	15	43	180	Dupont Fine Grain Industrial X-ray Film
10	10	54	175	Dupont Fine Grain Industrial X-ray Film
11	15	67	1020	Kodak Metal- lographic Plate
12	5	49	240	Kodak Metal- lographic Plate

\*All irradiations were at a neutron flux of  $2.38 \pm .1 \times 10^6$  n/cm<sup>2</sup>-sec.



Table 2 (Cont.)

Reactor Run No.	<u>Data</u>			
	Irradiation Time (Min.) <u>± .5 min.</u>	Decay Time (Min.) <u>± 1 min.</u>	Film Exposure Time (Min.) <u>± 1 min.</u>	Type of Film or Plate
13	10	81	133	Kodak Metal- lographic Plate
14	10	44	205	Kodak Metal- lographic Plate
15	20	50	190	Kodak Metal- lographic Plate
16	20	50	175	Kodak Metal- lographic Plate
17	10	29	110	Kodak Metal- lographic Plate
18	20	90	205	Kodak Metal- lographic Plate
19	20	40	170	Kodak Metal- lographic Plate
20	6	55	160	Kodak Metal- lographic Plate
21	6	55	130	Kodak Metal- lographic Plate
22	10	54	155	Kodak Metal- lographic Plate
23	20	79	140	Kodak Metal- lographic Plate
24	18	60	146	Kodak Metal- lographic Plate
25	20	64	144	Kodak Metal- lographic Plate
26	25	70	160	Kodak Metal- lographic Plate

Table 2 (Cont.)

Reactor Run No.	<u>Data</u>			
	Irradiation Time (Min.) <u>± .5 min.</u>	Decay Time (Min.) <u>+ 1 min.</u>	Film Exposure Time (Min.) <u>± 1 min.</u>	Type of Film or Plate
27	20	45	160	Kodak Metal- lographic Plate
28	20	101	480	Kodak Metal- lographic Plate
29	60	60	300	Kodak High Resolution Plate
30	30	62	193	Kodak Metal- lographic Plate

Table 3

Results

<u>Reactor Run No.</u>	<u>Sample Numbers</u>	<u>Results (all measured results are <math>\pm 0.001</math> inch)</u>
1	1A, 2A	No image on film
2	1A, 2A	No image on film
3	1A, 2A	No image on film
4	1A, 2A	No image on film
5	1A, 2A	No image on film
6	1A, 2A	No image on film
7	1A, 2A	No image on film
8	1A, 2A	No image on film
9	1A, 2A	No image on film
10	1A, 2A	No image on film
11	1A, 3B	No image on plate
12	1A, 2B	No image on plate
13	1A, 2B	No image on plate
14	1B, 2B	Faint sample images
15	1B, 3A	Sample images
16	1A, 2B	Sample images
17	1A, 2B	Sample images
18	1A, 1B	Some structure resolution of Sample 1A
19	2B, 3B	Sample images with no structure resolution
20	1A	No image on plate

Table 3 (Cont.)

Reactor Run No.	Sample Numbers	Results
		<u>(all measured results are <math>\pm</math> 0.001 inch)</u>
21	1A, 1B	No image on plate
22	1A, 2B	Sample images with no structure resolution
23	2C, 3A 1A 1B	No image resolution MR = .037 in. $D_o = 0.018$ in. $D_H = 0.021$ in. Little resolution
24	2A, 3B 1A 1B	No image resolution MR not measured $D_o = 0.00$ in. $D_H = 0.01$ in. No resolution
25	2A, 3A 1A	No image resolution MR not measured $D_o = 0.018$ in. $D_H = 0.014$ in.
26	2B, 3C 1A 1B	No image resolution MR = 0.030 in. $D_o = .008$ in. $D_H = .012$ in. MR = 0.027 in.
27	2B, 3C 1A 1B	No image resolution MR = 0.017 in. $D_o = .021$ in. $D_H = .033$ in. MR = 0.025 in.
28	2B, 3A 1A 1B	No image resolution MR = 0.029 in. $D_o = 0.00$ in. $D_H = 0.012$ in. MR = 0.028 in.
29	1A, 1B	No image on plate
30	1A 1C	MR = 0.21 in. $D_o = 0.019$ in. $D_H = 0.027$ in. MR = 0.026 in.

## V. Discussion

The following will consider the results listed in Table 3.

All of the samples were irradiated at various total flux levels; however, only the furnace cooled samples gave any radiographs or microradiographs of their structures. Therefore, the air-quenched and drop-cooled samples (Fig. 9) are ignored within this discussion.

Fig. 10 is a radiograph of cadmium turnings surrounded by tin flakes both of approximately 0.01 of an inch thickness. The dark cadmium turnings are evident upon the print while those of the tin are not visible. This radiograph demonstrates the difference between the neutron absorption cross-sections of cadmium and tin ( $2450 \pm 50^*$  and  $0.625 \pm .015^*$  barns, respectively).

The first ten reactor runs will be described briefly as they have little importance within the thesis. These runs were attempted using films which has a different resolution and sensitivity than metallographic plates.

The reactor runs, one to five inclusive, were performed using spectroscopic 649-0 film for the radiograph. These films have an extremely high (greater than 2000 lines/mm) resolution but a low sensitivity. This low sensitivity did not allow film exposure from the indium recorder sheets even at the saturation activity of the indium. Therefore, the use of this film was discontinued after the fifth reactor run.

Dupont Fine Grain Industrial X-ray film was used during reactor runs six to ten. The x-ray film has a higher sensitivity with a corresponding lower resolution than the spectroscopic 649-0. The

\*Handbook of Chemistry and Physics, Chemical Rubber Publishing Company, 44 Edition, 1963.

sensitivity of this film was such that resolution of the grain structure was not possible. However, the film did reveal differences in thickness of greater than 20 microns (approximately .001 inches) within the samples.

From the ten previous attempts at neutron microradiography, it was determined that resolution of the structure of the Cd-Sn alloy using indium as the transfer media would require an emulsion with a resolution and sensitivity between that of the 649-0 spectroscopic and the industrial x-ray film. The plate chosen to meet these requirements was the Kodak Metallographic which has a resolution of approximately 100 lines/mm.

The metallographic plates of reactor runs 11 to 13 exhibited no evidence of exposure from the indium plate. This was due to the small indium activity.

A faint image was present on the plate from reactor run 14. The image was entirely of the indium transfer sheet with no image of the sample present.

On the 15th experiment an image of the samples (one furnace cooled and one air cooled) was present. However, there existed no resolution of the grain structure on the metallographic plate (Fig. 11). The sample on the right in Figure 11 was 1B and on the left was 3C.

The image produced from the 16th attempt was an overexposed picture of the transfer sheet without a sample image. The overexposure was due to the long reactor run which caused a high indium activity.

A light transfer sheet image was present without the sample image for run 17. The combination of the results of runs 15 through 17

indicated that better results would be obtained if an irradiation of 20 minutes ( $2.86 \times 10^9$  n/cm<sup>2</sup>) at a flux level of  $2.38 \times 10^6$  was performed and if the decay time was about fifty minutes.

Run 18 yielded an image of the sample 1A with certain areas of structure resolution of sample 1 (Fig. 12 and 13). A comparison photomicrograph of the sample is Fig. 14. The areas of the sample which were resolved were the longer grains. The dark areas are Cd-rich and the light are Sn-rich. There were also dark areas too large and of the wrong geometry to be grains; therefore, they were areas of a cadmium enrichment not detectable by metallographic procedures. In the center of the sample there appeared a large flaw; metallography shows there is this flaw but does not give a picture of its true extent. Fig. 13, the 2X neutron radiograph, shows a distinct loss of resolution as compared to the radiograph. This is primarily due to the poor contrast or fog in the negative. The resolution was not measured because of the poor contrast and small areas of definable resolution.

The radiograph from reactor run 19 was overexposed due to a short decay time (40 minutes) and a long exposure time. In appearance it resembled reactor run 15 (Fig. 11).

Reactor runs 20 and 21 produced no sample images on either of the respective plates. This was due to the short irradiation time (6 minutes) given the irradiation assemblies.

As the irradiation time of runs 20 and 21 was short, the time for run 22 was increased to 10 minutes. This time proved to be too short to allow any visible structure resolution to appear. However, a faint sample image was apparent on the metallographic plate, identical in appearance to that of reactor run 15 (Fig. 11).

Reactor run 23 produced a neutron radiograph (Fig. 15) of sample 1A with a greater amount of resolution than that of reactor run 18. However, the maximum visible resolution was only .039 inches; the radiograph was also limited by the amount of fog, or background grayness, of the negative as was that of reactor run 18. The micro-radiograph (Fig. 16) showed less resolution due to lack of contrast. The white "hooks" which appear are emulsion flaws, not grain structure.

The fog on the negative also limits the actual resolution in that it tends to broaden the grain boundaries. The distances,  $D_o$  and  $D_H$ , measure between cadmium rich areas and were used as inverse measures of the lack of contrast or fog. As these distances increase, i.e., the boundaries appear sharper, the contrast increases and the background decreases. The distance measured within the horseshoe shaped grain ( $D_H$ ) in the metallograph was determined to be 0.021 inches.  $D_o$  was not distinguishable, and it was given a value of zero.

Reactor run 24 was performed using an irradiation time and decay time shorter than run 23. The structure (Fig. 17) was less distinct illustrating that the primary factors in neutron radiography (and micro-radiography) were the time of irradiation and the decay time. The resolution was comparable to that of run 18.  $D_H$  was 0.010 inches and  $D_o$  was again not measurable and was given a value of zero. The micro-radiograph (Fig. 18) gave a very faint resolution of the grain structure.

The results of reactor run 25 was considered with reservation because of use of a warm developer solution which caused a lack of contrast within the emulsion. This error caused a maximum visible resolution of only 0.020 inches to appear in the radiograph (Fig. 19). The  $D_H$  distance was 0.018 inches and the  $D_o$  measured was 0.014 inches.



In the previous experiments an optimum irradiation time of 20 minutes has been determined; in an attempt to eliminate the metallographic plate fogging, run 26 used an irradiation time of 25 minutes. The fog did not diminish noticeably (Fig. 20) and the resolution for sample 1A (.030 inches) was poorer than for run 23.  $D_o$  and  $D_H$  decreased to 0.008 and 0.012 inches, respectively, illustrating an increase in the lack of contrast. But the irradiation revealed cadmium rich areas of approximately .030 inches in diameter in sample 1B. Sample 1A, shown in the microradiograph (Fig. 21), showed little resolving. The small resolution was due to the longer decay time allowed.

Reactor run 27 was designed such that it would have the optimum contrast for samples 1A and 1B. This required an irradiation time of 20 minutes, a short decay time of 45 minutes, and an exposure time of 160 minutes. These criteria were determined from the previous runs as those which would give maximum resolution. For sample 1A the radiograph exhibited a resolution of 0.017 inches (Fig. 22).  $D_o$  and  $D_H$  were 0.021 inches and 0.033 inches, respectively. The 3X neutron microradiograph (Fig. 23) of sample 1A showed a loss of contrast on enlarging and its resolution was 0.100 inches. For sample 1B the resolution obtained was 0.025 inches. The 5X microradiograph (Fig. 24) demonstrated a loss in resolution when compared to Figure 23.

Reactor run 28 (Fig. 26) was performed to see if variations of the decay time would cause a distinctive change in the maximum visible resolution. The change in the decay time was from 45 minutes (run 27) to 101 minutes. There was a great loss of maximum resolution, to .029 inches from .017 (run 27) due to the change in decay time in sample 1A.

The  $D_o$  distance was 0.00\*inches and  $D_H$  distance was 0.012 inches. The maximum resolution of sample 1B was 0.028 as compared to .025 for run 27. The microradiograph (Fig. 27) of sample 1A was indistinct.

Reactor run 29 used a high resolution plate (2000 lines/mm) in an attempt to gain greater resolution. The attempt failed because of the low sensitivity of the plate; there was no exposure of the plate.

Reactor run 30 (Fig. 28 and 29) was performed with a longer irradiation time, decay time, and exposure time as a test for a poorer resolution. The resolution (.021 inches) decreased from that of run 27 (.017 inches) for sample 1A.  $D_o$  was 0.019 inches and  $D_H$  was 0.027 inches. This run also included sample 1C which, metallographically, was identical in grain, size and texture to sample 1B. The maximum resolution obtained, of this sample, was 0.026 inches. Figure 30 is a neutron micrograph of sample 1C. Figures 31 and 32 are microradiographs of sample 1A.

The radiation hazard involved in the handling of the radioactive indium imposed certain restrictions upon the irradiation and decay times for each run. The Atomic Energy Commission has maximum permissible dose limits of 75 rem/year for the hands and feet and 5 rem/year or 20 mr/day for the entire body.

The principle hazard was to the hands, but, as a safety factor, the dosage received per day was held below the daily whole body dose. Thus, the irradiation and/or the decay times were of a duration which would give a dosage of 5 mrem or less during the 10 minute handling time after each run. In this manner, the investigator never received more than 15 mr/day.

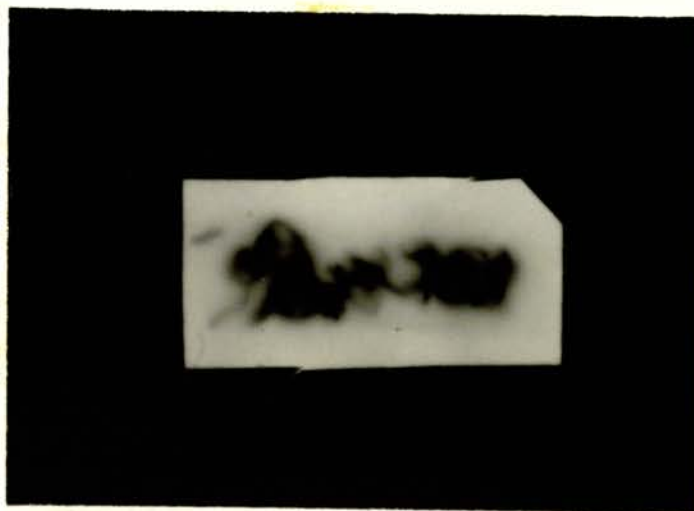
\*Indicates no visible boundary between two prongs on area 1.



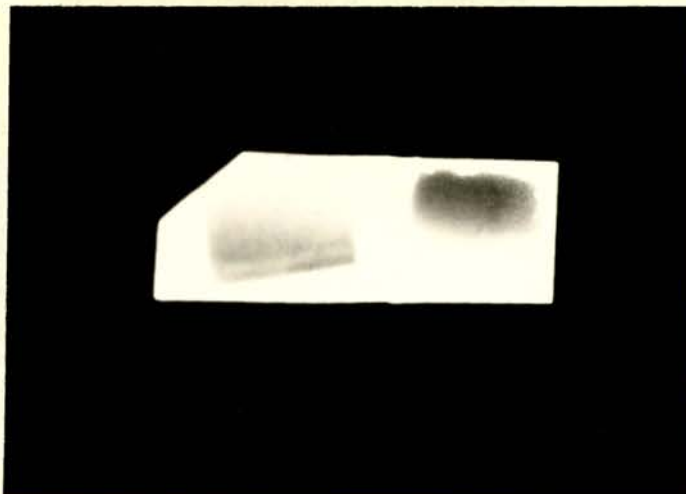
Sample 2A

Sample 3A

Reactor Run 27  
Figure 9



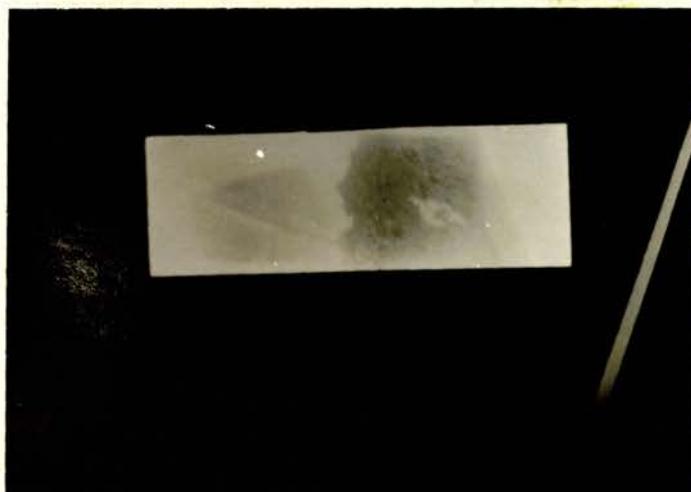
Cadmium and Tin Turnings  
Figure 10



Sample 1B

Sample 3C

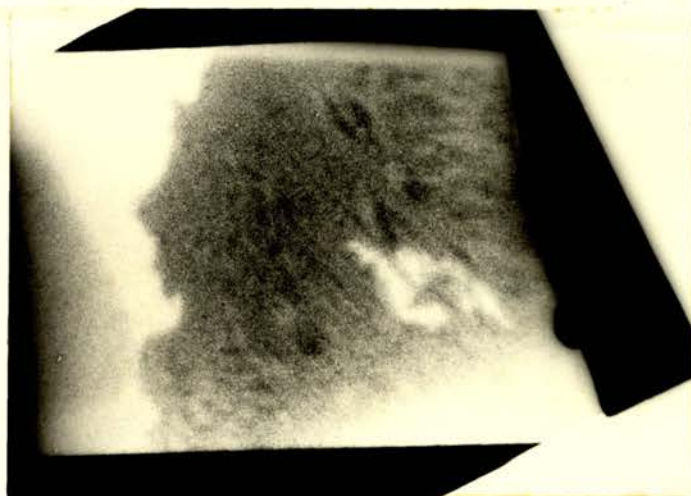
Reactor Run 9  
Figure 11



Sample 2C

Sample 1A

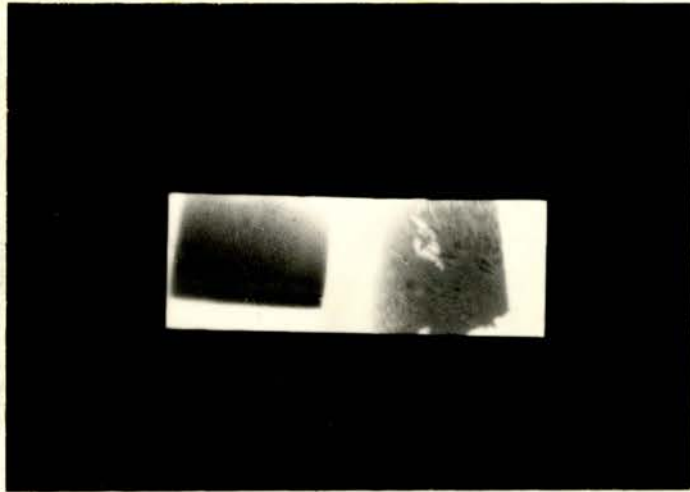
Reactor Run 18  
Figure 12



Sample 1A 2X  
Reactor Run 18  
Figure 13



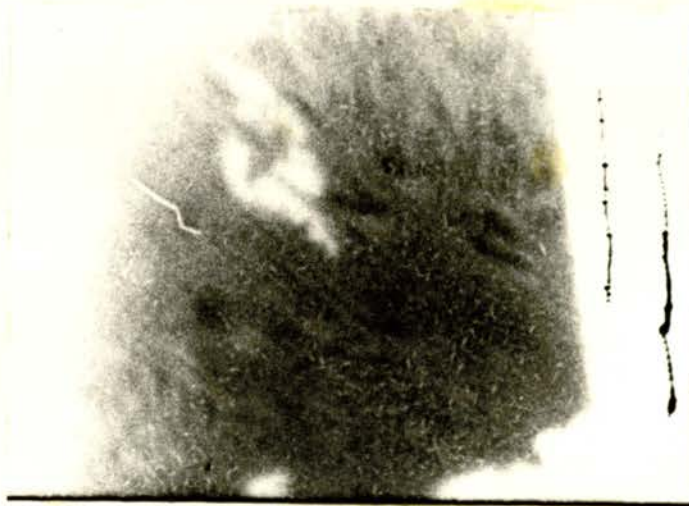
Sample 1A 1.5X  
Reactor Run 18  
Figure 14



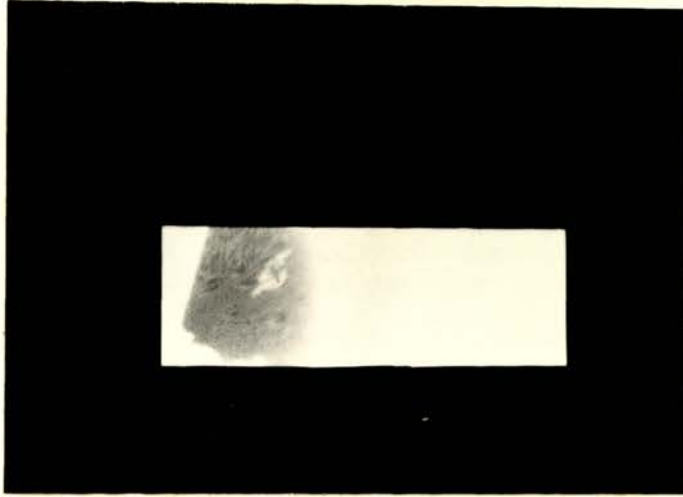
Sample 1B

Sample 1A

Reactor Run 23  
Figure 15



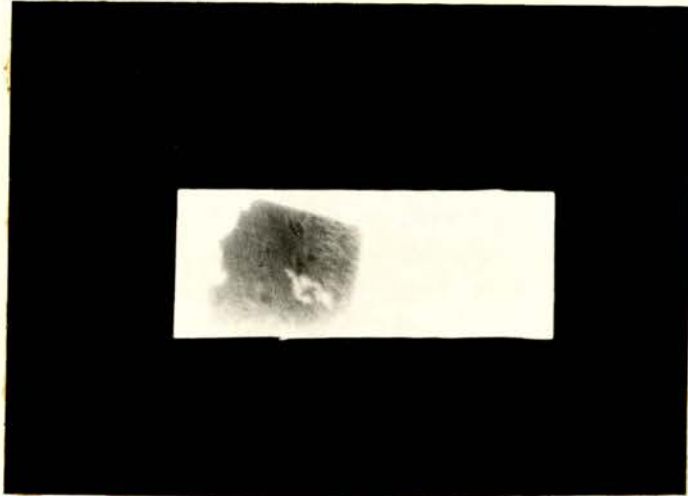
Sample 1A 3X  
Reactor Run 23  
Figure 16



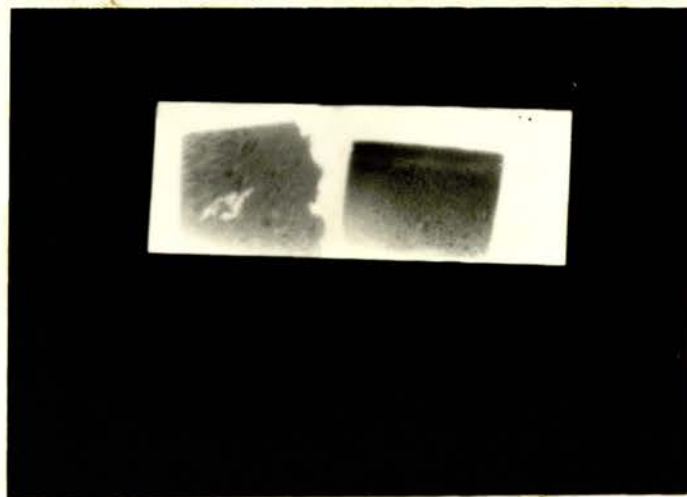
Sample 1A  
Reactor Run 24  
Figure 17



Sample 1A 3X  
Reactor Run 24  
Figure 18

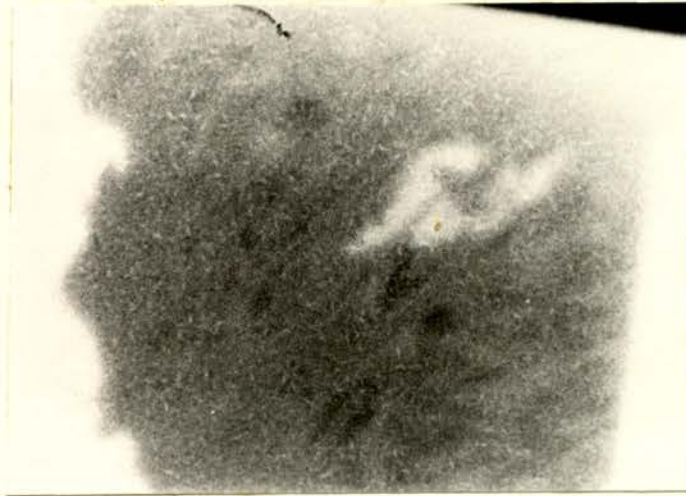


Sample 1A  
Reactor Run 25  
Figure 19

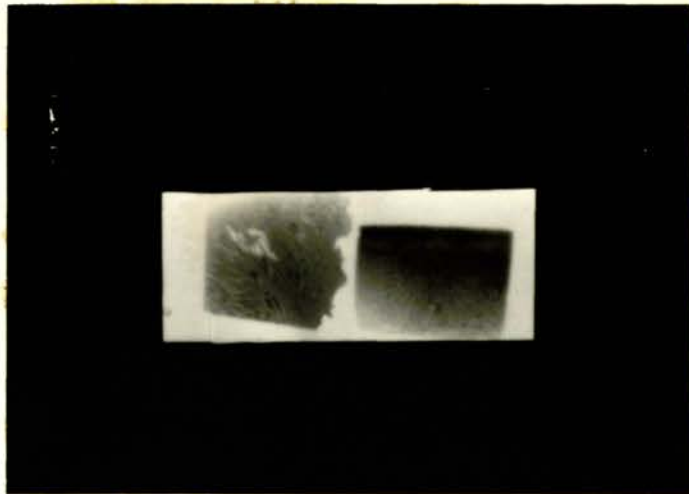


Sample 1A                      Sample 1B  
Reactor Run 26  
Figure 20





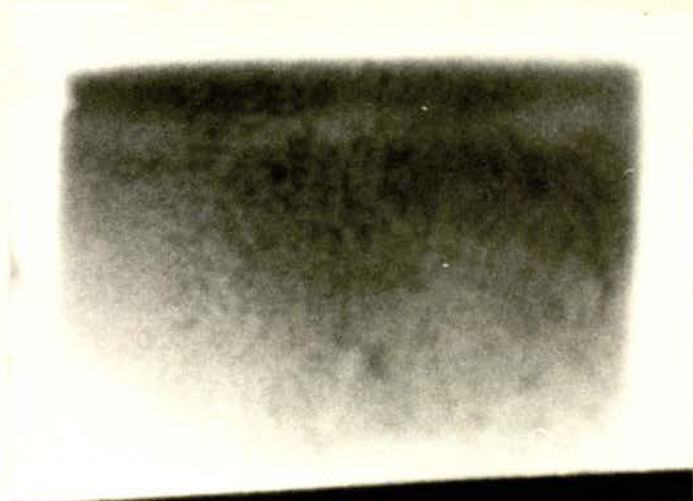
Sample 1A 3X  
Reactor Run 26  
Figure 21



Sample 1A                      Sample 1B  
Reactor Run 27  
Figure 22



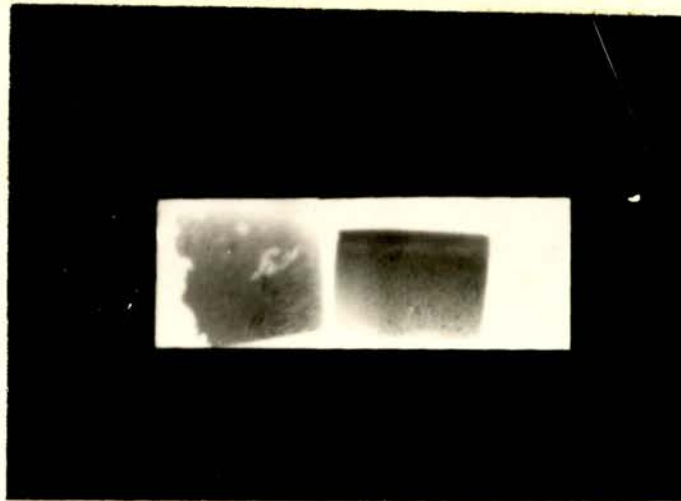
Sample 1A 3X  
Reactor Run 27  
Figure 23



Sample 1B 3X  
Reactor Run 27  
Figure 24



Sample 1A 5X  
Reactor Run 27  
Figure 25



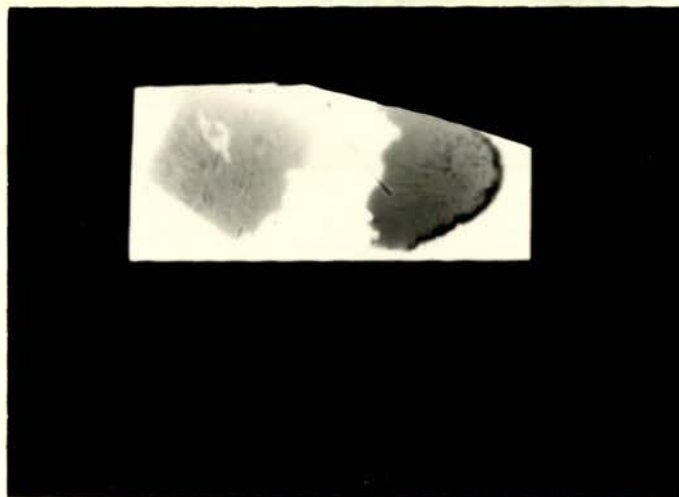
Sample 1A

Sample 1B

Reactor Run 28  
Figure 26



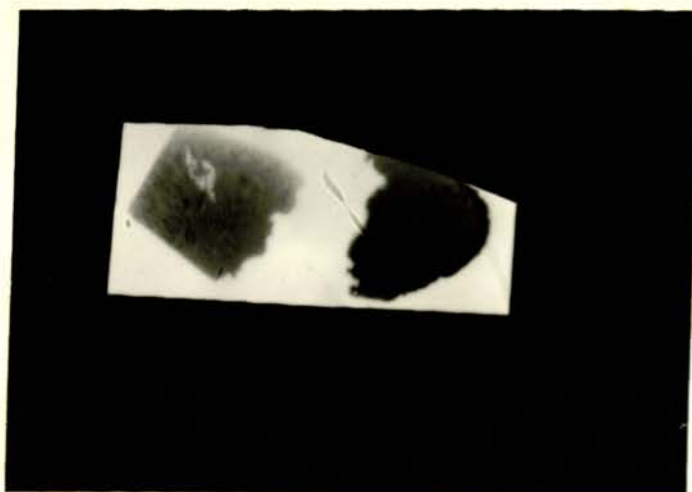
Sample 1A 3X  
Reactor Run 28  
Figure 27



Sample 1A

Sample 1C

Reactor Run 30  
Figure 28



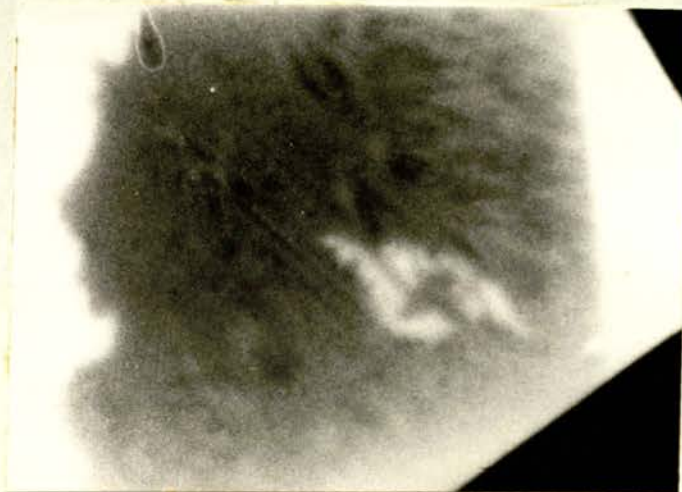
Sample 1A

Sample 1C

Reactor Run 30  
Figure 29

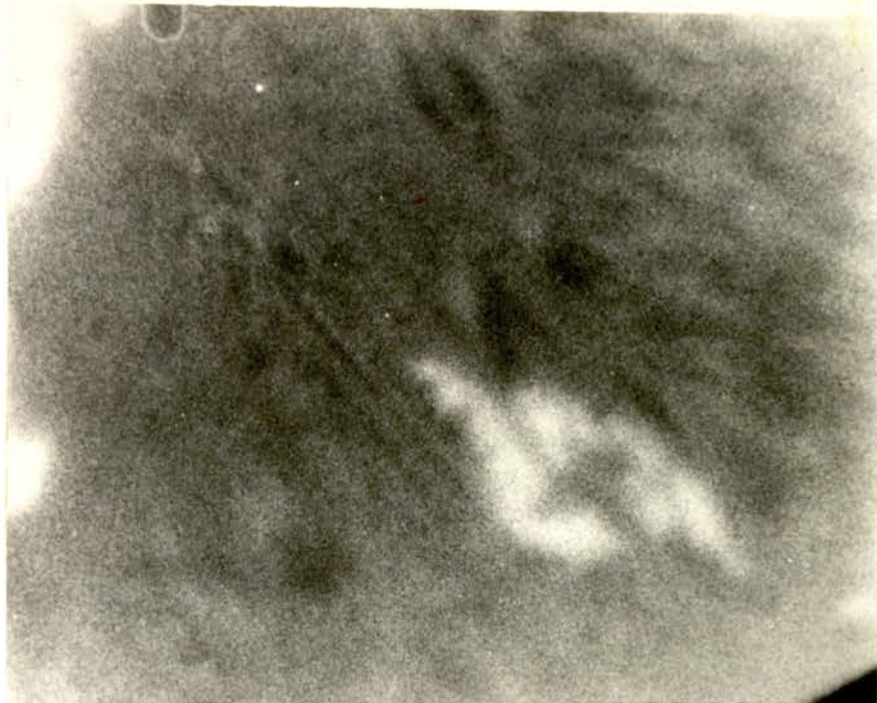


Sample 1C 3X  
Reactor Run 30  
Figure 30



Sample 1A 3X  
Reactor Run 30  
Figure 31





Sample 1A 5X  
Reactor Run 30  
Figure 32

## VI. Conclusion

The maximum resolution obtained was 0.017 inches on the radiograph of run 27. No grains were ascertained which were of a diameter smaller than 0.012 inches on this radiograph. However, from the literature review, it was determined that grains of a size approximately equal to the thickness of the sample should have been in evidence. The thickness of sample 1A was 0.0049 inches; there was no evidence of grains of this diameter within any of the radiographs or microradiographs. From this discovery, it was concluded there was a limiting factor which prevented a resolution of less than 0.017 inches for this alloy. The factors considered possibly responsible for the resolution limit were:

(1) position of the sample, (2) flatness of the indium recorder sheet, (3) position of the indium transfer sheet upon the metallographic plate, (4) the resolving capability of the plate, and/or (5) the  $4\pi$  beta particle and photon emission from the activated indium nuclei.

Poor positioning of the sample on the indium was rejected because of the glass slide used to firmly hold the sample in place. As the samples were flat and rigid, this insured complete contact if the indium was flat.

The flatness of the indium sheet was checked by examining an indium transfer sheet under a 10X microscope. The maximum flaws corresponded to small scratches less than 0.006 inches long. As there were large flat areas evident containing no scratches, this supposition was also rejected.



The positioning of the indium transfer sheet upon the metallographic plate as a cause of limited resolution was rejected. The weight of the aluminum backing plate insured the intimate contact of the indium and the emulsion.

The resolution of a metallographic plate is approximately 100 lines/mm (2540 lines/inch). The resolution of the plate was capable of resolving the grains which should have been in evidence.

The fifth possible factor,  $4\pi$  emission of photons and beta particles, was considered the most probable cause of the limited plate resolution. A cadmium rich particle in contact with a similar tin rich area was considered in intimate contact with an indium recorder plate; then, after a period of irradiation and decay, the indium behind the cadmium rich area (region 1) would have less activity than the indium behind the tin rich area (region 2). However, when the indium was placed on an emulsion, each activated nuclei would emit a beta particle and an average number of photons randomly over all directions. As the particles were randomly emitted, a definite percentage of those emitted within each region would penetrate the emulsion under the other region. Considering region 2 would be emitting more particles, then region 2 particles must have been contributing more exposure of the emulsion under region 1 than vice versa. Therefore, a more radioactive region would tend to darken adjacent areas of an emulsion which were under a less active source.

Region 1 was then considered to have a region 2 on both sides and region 1 was slowly reduced in width, at a certain width region 1 would not be detected upon the emulsion. The particles from the adjacent regions which struck the emulsion of region 1 would be of a magnitude such that there would be no detectable exposure. The size of the region 1 area at

the limit of detectability was the "critical size" and can be considered the reason for the limited resolution of the sample 1A radiographs and microradiographs. This also indicates that for a given transfer sheet, there is a definite limit on the resolution obtainable holding all factors except time constant.

The "critical size" would also be related to the contrast of the adjacent areas. In Appendix 4 it is shown that the contrast is a maximum when the irradiation time is long and the decay time short.

The distances of  $D_o$  and  $D_H$  were measured for a somewhat quantitative measure of the contrast within the plate. Although there were not enough results, statistically, to justify a firm conclusion, there was a general tendency for  $D_o$  and  $D_H$  to improve, i.e., increase, as the irradiation time lengthened and/or the decay time shortened. The boundaries also became much easier to see as the contrast increased.

The fog or lack of contrast inherent within the neutron radiographs and microradiographs was due to two types of radiation. The localized radiation, beta particles, was the primary cause of distortion and pseudoenlargement of the grains with the structures. The long range particles, photons, were the cause of the general fog which extended across the plate reduced the ability to enlarge the neutron radiograph.

## VII. Summary

The summation of the results demonstrates that neutron microradiography to a certain critical grain size is possible. The critical grain size found under the conditions of the UMR Reactor was found to be under 0.017 inches. However, under ideal conditions of an indium saturated activity, zero decay time, and a long film exposure time using a film of approximately 600 lines/mm resolution capability, the resolution obtainable should be under 0.001 inches which would be useful for certain large-grained alloys. As an extremely high resolution technique neutron microradiography is not feasible.

The limitation on neutron microradiography was primarily the lack of contrast caused by the  $4\pi$  beta particle and photon emission from the activated nuclei. The fog caused by the beta particles was somewhat controlled by variations in the irradiation and decay times. The increase in the irradiation time or decrease in the decay time caused a noticeable increase in the resolution and contrast of the radiograph or microradiograph. The gamma ray or photon has a longer range than the beta particle. For this reason, the lack of contrast caused by the photons caused a poor resolution of the neutron microradiographs.

### VIII. Recommendations

The experiment should be performed with enough replications to give a statistical analysis of the possible resolution. Repeated runs at specified times would enable the investigator to form more accurate conclusions concerning the maximum resolution obtainable.

Different recorder sheets such as dysprosium and silver could be used in place of indium. The different cross-sections and half lives should change the maximum resolution considerably.

In other evaluations, plates of higher resolution ( 600 lines/mm) should be used. These plates will require a special order.

## IX. Appendix 1

### Materials

The materials essential to this investigation are listed below.

Cadmium Pellets. 10 pounds of 99.9+% cadmium pellets supplied by the American Smelting and Refining Company, St. Louis, Missouri.

Tin Ingots. 5 one pound ingots of 99.99+% purity produced by Fisher Chemical Company, Pittsburg, Pennsylvania.

Indium Sheets. 30 4" x 4" x .01" sheets supplied by the Indium Corporation of America, New York, New York.

Alumina. One pound of Linde B alumina.

### Equipment

The equipment essential to this investigation are listed below.

Furnace. One 800°C electric furnace.

Aluminum Plates. 8 metallographically polished 1" x 2" x 1/4" aluminum plates.

Hand Grinder. 600, 400, 360, 240 Si-C grit grinder.

Polishing Wheel. One 8 inch polishing wheel whit billiard cloth.

Microscope Slides. 14 1" x 2" microscope slides.

Recorder Sheets. (Appendix 5).

Gum Bands. 50 No. 2 gum bands.

UMR Reactor. (Appendix 6).

Photographic Plates and Film. 72 Kodak Metallographic Plates, 40 inches of Kodak Type 649-0 Spectroscopic Film, and 1 box of Dupont Fine Grained Industrial X-ray Film.

Microscope. 10X microscope with scale of 0.011 mm.

Enlarger. Leitz Focomatic enlarger.

Lens. El Nikon 5 cm f/2.8 lens.

Miscellaneous supplies include darkroom supplies, radiation handling equipment, and sample handling equipment. Other materials are charcoal and Canada balsam.

X. Appendix 2Example Calculation of Sample Thickness

Sample 1B

Density\* = 7.70 gm/cc

Area = 2.60 cm<sup>2</sup>

Mass = 0.3321 gm

Average Thickness =  $\frac{\text{mass}}{\text{area} \times \text{density}}$

$$= \frac{3321 \text{ gm}}{2.60 \text{ cm}^2 \times 7.70 \text{ gm/cc}}$$

$$= 0.0067 \text{ inches}$$

\*Handbook of Chemistry and Physics, Chemical Rubber Publishing Company,  
44 Edition, 1963

XI. Appendix 3

Calculation of Flux at Sample Surface

$$\phi_{\text{thermal}} = \frac{G - B}{FK(1 - e^{-\lambda t_1}) (1 - e^{-\lambda t_3}) e^{-\lambda t_2}}$$

where:

G = foil counts = 10236 units/minute

B = background = 80 units/minute

F = Au foil factor = 1.197

K = counter constant = 359

t<sub>1</sub> = irradiation time at 10 Kw = 30 minutes ± 20 seconds

t<sub>2</sub> = decay time = 58 minutes ± 3 seconds

t<sub>3</sub> = counting time = 10 minutes ± 1 second

λ = decay constant = 2.97 x 10<sup>-6</sup> seconds<sup>-1</sup>

$$\phi_{\text{thermal}} = \frac{10156}{1.197(359) (1 - e^{-5.37 \times 10^{-3}}) (1 - e^{-1.79 \times 10^{-3}}) \times e^{-1.04 \times 10^{-2}}}$$

$$= \frac{10156}{(1.197) (359) (1 - .995) (1 - .998) (.990)}$$

$$= \frac{10156 \times 10^2}{(1.197) (359) (.005) (.002) (.990)}$$

$$= 2.38 \times 10^6 \text{ n/cm}^2/\text{sec} \pm 4\%$$



XII. Appendix 4

Factors Affecting Contrast

Consider two equal-sized adjacent circles of which one is cadmium rich material, the other tin rich. The areas have the same thickness. The activity buildups of the indium areas in contact with the circles is defined by the following equations.

$$\text{Indium activity behind cadmium rich area} = A_1' = K_1 (1 - e^{-\lambda t_1})$$

$$\text{Indium activity behind tin rich area} = A_2' = K_2 (1 - e^{-\lambda t_1})$$

where:

$K_1$  = constant

$K_2$  = constant

$t_1$  = time of irradiation

$\lambda$  = decay constant of indium

Now at a certain time,  $t_1$ , the irradiation is halted and the activity, of each of the indium areas, are allowed to decay as:

$$\text{(cadmium rich)} \quad A_1'' = A_1' e^{-\lambda t_2}$$

$$\text{(tin rich)} \quad A_2'' = A_2' e^{-\lambda t_2}$$

where:

$t_2$  = the time from irradiation.

Then the activity upon the film or plate, at any time,  $t$ , from each of the areas must be:

$$\text{(cadmium rich)} \quad A_1 = C_1 A_1'' e^{-\lambda t_3}$$

$$\text{(tin rich)} \quad A_2 = C_2 A_2'' e^{-\lambda t_3}$$

$t_3$  = time of film exposure

$C_1$  and  $C_2$  = fractions concerning  $4\pi$  emission. For perfect circles  $C_1 = C_2$ .

If the exposure is considered to be linear with respect to the number of particles striking it, then let the maximum exposure of the plate be  $D_2$ . The maximum exposure will occur from the indium which was in contact with the tin rich area as it is more radioactive. Therefore:

$$D_2 = Q \int_{t_3} A_2 dt$$

where:

$Q$  = units constant

$$Q \int_{t_3} A_2 dt = Q \int_{t_3} C_2 A_2'' e^{-\lambda t_3} dt$$

$$D_2 = Q C_2 A_2'' (e^{-\lambda t_3} - 1)/(-\lambda)$$

$$= Q C_2 A_2' e^{-\lambda t_2} (e^{-\lambda t_3} - 1)/(-\lambda)$$

$$= Q C_2 K_2 (1 - e^{-\lambda t_1}) e^{-\lambda t_2} (e^{-\lambda t_3} - 1)/(-\lambda)$$

In a similar manner,  $D_1$  can be obtained.  $D_1$  will be less than  $D_2$  as  $D_1$  refers to the indium in contact with the cadmium rich area.

$$D_1 = Q C_1 K_1 (1 - e^{-\lambda t_1}) e^{-\lambda t_2} (e^{-\lambda t_3} - 1)/(-\lambda)$$

The difference between  $D_2$  and  $D_1$  is proportional to the contrast obtained on a radiograph or microradiograph.

$$D_2 - D_1 = D = \left(\frac{QC}{-\lambda}\right) (K_2 - K_1) (1 - e^{-\lambda t_1}) e^{-\lambda t_2} (e^{-\lambda t_3} - 1)$$

From the above equation it is easily seen that the contrast of the plate increases as the irradiation time ( $t_1$ ) approaches infinity, as the decay time ( $t_2$ ) approaches zero, and as the exposure time ( $t_3$ ) approaches infinity.

The irradiation runs for the thesis research gave the following values for maximization of the contrast with consideration from the health physics standpoint.

$$1 - e^{-\lambda t_1} = 1 - e^{-1.28 \times 10^{-2} \times 20} = .24$$

$$1 - e^{-\lambda t_3} = 1 - e^{-1.28 \times 10^{-2} \times 160} = .87$$

$$e^{-\lambda t_2} = e^{-1.28 \times 10^{-2} \times 45} = .56$$

By increasing the irradiation time and decreasing the decay time, the contrast could be raised by a factor of 8. This would allow the resolution to approach 0.002 inches using indium as the transfer sheet.

XIII. Appendix 5

The indium transfer sheets were made by shearing 4 inch x 4 inch squares of 0.010 inches thick indium sheets into 1 inch x 2 inch sections. These sections were then mounted onto 1 1/2 inch x 2 1/2 inch x 1/4 inch metallographically polished aluminum plates. Canada balsam was used to seal each section to the aluminum plate with intimate contact. The balsam was applied at 100°C and allowed to harden around the edge of each indium section.

XIV. Appendix 6

The University at Rolla Reactor is a 10 Kw heterogeneous, thermal, pool-type, research and training reactor. The pool is 9 feet wide, 19 feet long, 27 feet deep and holds approximately 32,000 gallons of high purity water.

The core is on a heavy aluminum grid plate suspended from the bridge spanning the pool. The core fuel elements are 3 inches x 3 inches x 36 inches and contains 10 fuel plates about 1/16 inches thick. Each plate is an aluminum-uranium oxide-aluminum sandwich with 17 grams of Uranium-235. The control elements are similar but with only 6 fuel plates which allows the insertion of one of the safety rods or the regulating rod in the center.

The chief feature of this reactor with regard to this thesis is the graphite thermal column. The thermal column consists of 4 inches x 4 inches graphite stringers which form a 4 feet x 4 feet x 5 feet (away from core) parallelepiped.

The core side of the thermal column has lead as a gamma shield. The shield door to the column is concrete approximately 5 feet long. The flux at the interior of the shield is approximately  $2.38 \times 10^6$  n/cm<sup>2</sup>/sec.

XV. Appendix\* 7

<u>Isotope</u>	<u>% National Abundance</u>	<u>Half-Life</u>	<u>Mode of Decay</u> <u>Radiation Energies in MEV</u>
In <sup>113</sup>	4.16	stable	
In <sup>114</sup> <sub>m</sub>		50 days IT	e <sup>-</sup> 0.192
In <sup>114</sup>		72 seconds	β <sup>+</sup> 0.65 β <sup>-</sup> 1.98 λ 0.715 0.548 K
In <sup>115</sup>	95.84	6 x 10 <sup>14</sup> years	β <sup>-</sup> 0.63
In <sup>116</sup> <sub>m</sub>		54 minutes IT	β <sup>-</sup> 0.6 0.87 1.00 λ 1.274 1.085 2.09 0.406 1.487
In <sup>116</sup>		13 seconds	β <sup>-</sup> 2.95

## Nomenclature:

β<sup>-</sup> beta particleβ<sup>+</sup> positron

λ gamma ray

e<sup>-</sup> internal electron conversion

K orbital electron capture

IT isomeric transition

m denotes different energy level

The cross section for the production of the products of  $\text{In}^{113}$  under thermal neutron bombardment are  $56 \pm 12$  and  $2.0 \pm 0.6$  barns with reference to  $\text{In}^{114}$  and  $\text{In}^{114m}$ , respectively. That for the products of  $\text{In}^{115}$  under thermal neutron irradiation are  $155 \pm 10$  and  $52 \pm 6$  barns with reference to  $\text{In}^{116m}$  and  $\text{In}^{116}$ , respectively. For consideration in neutron microradiography, all product isotopes with the exception of  $\text{In}^{116m}$  may be neglected due to half-life and/or cross-section.

XVI. Bibliography

1. Maddigan, S.E., Journal of Applied Physics, 15, 43, (1944).
2. Spronll, W. T., "X-rays in Practice", McGraw-Hill, (1946).
3. "Radiography in Modern Industry", Eastman Kodak, (1941).
4. Taylor, A., "An Introduction to X-ray Metallography", Chapman and Hill, (1949).
5. Sharpe, R. S., "The Microradiography of Metals: Its Advantages and Limitations", Proceedings of a Symposium held at the Cavendish Laboratory, Cambridge, 1956, Oxford Press, (1956).
6. Straumanis, M.E.: Personal Correspondence.
7. Votava, E., Berghazan, A., and Gillette, R.H., "Microradiography in Some Metallurgical Problems", Proceedings of a Symposium held at the Cavendish Laboratory, Cambridge, 1956, Oxford Press, (1956).
8. Berger, Harold, "A Summary Report on Neutron Radiography", ANS-6846, (July, 1964).
9. Beck, C. N.: Personal Correspondence.



XVII. Vita

The author was born October 11, 1942 in Phillipsburg, Kansas. He received his elementary education at Phillipsburg Grade School, Phillipsburg, Kansas and Vance Grade School, District 135, Chariton County, Missouri. He received his secondary education at Glasgow High School, Glasgow, Missouri, and Keytesville R-3, Keytesville, Missouri. He graduated with a Bachelor of Science in Metallurgical Engineering (Nuclear Option) from the University of Missouri School of Mines and Metallurgy in May, 1963.

He has been enrolled in the Graduate School of the University of Missouri at Rolla since September, 1963 and has been a Nuclear Science and Engineering Fellow for the period of September, 1963 to May, 1965.